

Gas-Phase Formation of Radical Cations of Monomers and Dimers of Guanosine by Collision-Induced Dissociation of Cu(II)–Guanosine Complexes

Ping Cheng and Diethard K. Bohme*

Department of Chemistry, Centre for Research in Mass Spectrometry and Centre for Research in Earth and Space Science, York University, Toronto, Ontario, Canada, M3J 1P3

Received: March 9, 2007; In Final Form: July 6, 2007

An electrosprayed water/methanol solution of guanosine and $\text{Cu}(\text{NO}_3)_2$ was observed to give rise to gas-phase copper complexed ions of $[\text{CuL}_n]^{2+}$, $[\text{CuL}(\text{MeOH})_n]^{2+}$, and $[\text{CuG}_n(\text{NO}_3)]^{*+}$, as well as the ions $[\text{L}]^{*+}$, $[\text{L} + \text{H}]^+$, $[\text{G}]^{*+}$, and $[\text{G} + \text{H}]^+$ ($\text{L} = \text{guanosine}$, $\text{G} = \text{guanine}$). The Collision-Induced Dissociation (CID) of $[\text{CuL}_3]^{2+}$ and $[\text{CuL}(\text{MeOH})_n]^{2+}$ ($n = 2, 3$) generates guanosine radical cations $[\text{L}]^{*+}$, while dimeric guanosine radical cations $[\text{L}_2]^{*+}$ are generated in the dissociation of $[\text{CuL}_4]^{2+}$. Protonated guanosine $[\text{L} + \text{H}]^+$ is one of the main products in the primary dissociation of $[\text{CuL}_2]^{2+}$, while the dissociation of the higher-order $[\text{CuG}_2]^{2+}$ produces the $[\text{G}]^{*+}$ radical cation. The guanosine dimer radical cation, $[\text{L}_2]^{*+}$ presumably arises from the interaction of two guanosine molecules via proton and hydrogen bonding and is observed to dissociate into $[\text{L} + \text{H}]^+$ and $[\text{L} - \text{H}]^*$ at low energies. We propose that the first two ligands bind strongly with Cu(II) through N7 and O6 to form a $[\text{CuL}_2]^{2+}$ complex with a four-coordinated planar structure and that a third ligand binds loosely with copper to form $[\text{CuL}_3]^{2+}$. Additional ligation observed in the formation of $[\text{CuL}_n]^{2+}$ ($n \leq 6$) ions is presumed to occur by hydrogen bonding. The ribose group of guanosine appears to play an important role in the stabilization of the doubly charged Cu–guanosine complex and in intraligand proton transfer upon CID. The molecular radical cations $[\text{L}]^{*+}$ observed in the ESI-MS spectrum at low declustering potentials originate primarily from $[\text{CuL}(\text{MeOH})_{2,3}]^{2+}$ complexes which can dissociate more easily than $[\text{CuL}_3]^{2+}$.

1. Introduction

Metal cations can both stabilize and destabilize DNA.^{1,2} In particular, the interaction of divalent cations with nucleic acids plays an important role in promoting and maintaining their functionalities.^{1–4} The biologically important d^9 open shell Cu^{2+} cation has a rich redox chemistry and is closely associated with DNA bases,^{5,6} particularly guanine. Most studies have emphasized that the exposure of DNA to Cu^{2+} can have different consequences such as single and double strand cleavage, base modification, and formation of abasic sites.^{7,8} So the nature of the interactions of Cu^{2+} with nucleoside bases should be understood in order to unravel the mechanism for such damage. The interactions and the coordination chemistry of metal cations with nucleosides and nucleotides have been studied quite extensively in the liquid phase with NMR, X-ray, and other technologies,^{2,5,9–14} but no data appear to be available for the intrinsic gas-phase behavior of such interactions.

Metal–ligand complexes can be generated and examined in the gas phase with electrospray ionization mass spectrometry (ESI-MS).^{15–17} Since the early 1990s, ESI-MS has become the most frequently used technique for the study of the gas-phase complexes of monovalent and divalent metal cations with a variety of protic and aprotic ligands, including water,^{18–22} alcohols,^{23–25} acetone and other ketones,^{18,23,26} acetonitrile,^{24,27} pyridine,^{16,24} dimethyl sulfoxide,^{15,23,28} and some DNA bases.^{29–34} Recently, the study of gas-phase copper complexes has grown into an active and promising research area. For example, gas-phase copper complexes of amino acids have been used to

distinguish isomeric and isobaric amino acids.³⁵ The fragmentation of $[\text{Cu}(\text{L})(\text{M})]^{2+}$ complexes, where M is typically an oligopeptide containing the tryptophan or tyrosine residue and L is an auxiliary tridentate ligand, has been used to generate M^{*+} radical cations,^{36–38} as well as peptide³⁹ and nucleoside radical cations.⁴⁰ Very recently, Ke et al.⁴¹ observed the stable dimeric radical cations of tryptophan and tyrosine derivatives in the CID of $[\text{Cu}(\text{dimethylenetriamine})(\text{amino-acid derivatives})_2]^{2+}$.

Here we report results of an investigation of the gas-phase interaction of Cu^{2+} with the nucleotide guanosine using ESI mass spectrometry. Complexes of Cu^{2+} and guanosine were formed in solution and electrosprayed into the gas phase. The stabilities of these complexes were assessed with measurements of their fragmentation as induced by collisions with nitrogen molecules. The observed fragmentation channels include formation of monomeric and dimeric ligand radical cations via intramolecular electron transfer (ET), formation of protonated ligands via intramolecular proton transfer (PT), ligand elimination, ligand dissociation, and ligand dissociation accompanied by charge reduction.

2. Experimental Method

The experiments were performed with a commercial MDS SCIEX (Concord, ON, Canada) API 2000 prototype triple-quadrupole ($\text{Q}_1\text{q}_2\text{Q}_3$) mass spectrometer equipped with an ESI source. The operating conditions were as follows: ESI in the positive ion mode; ion spray voltage, 5500 V; ring-electrode potential, 300 V; a range of potentials between the orifice and the skimmer (the declustering potential); curtain gas (N_2) flow

* Address correspondence to this author. E-mail: dkbohme@yorku.ca. Phone: 416-736-2100, ext 66188. Fax: 416-736-5936.

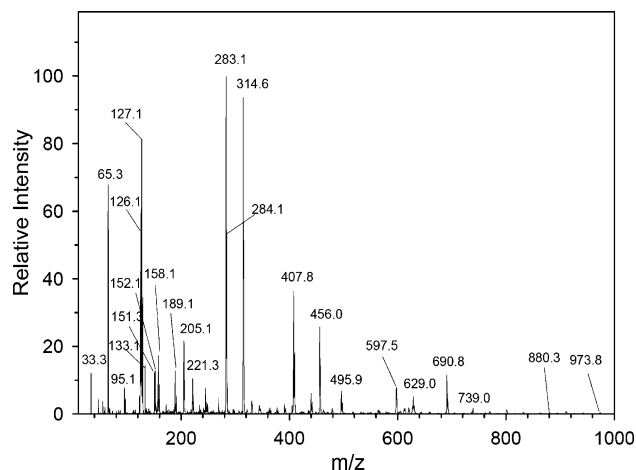


Figure 1. ESI mass spectrum of a water/methanol solution of Cu^{II} (0.1 mM) and guanosine (0.2 mM) at a low declustering potential (15 V).

rate, 10 arbitrary instrument units; nebulizer gas flow rate, 20 arbitrary instrument units dry air; and sample flow rate, $5 \mu\text{L min}^{-1}$.

MS/MS was performed in the product ion monitoring mode with N_2 as collision gas.⁴² The first quadrupole (Q1) was used to select the precursor ions and the dissociation was induced by collisions in the second quadrupole (q2). The product ions were mass analyzed in the third quadrupole (Q3). The laboratory collision energies (E_{lab}) were typically 10–50 eV. The nominal collision voltage for the instrument begins at 5 V. The kinetic energy distribution of the parent beam was not determined.

$\text{Cu}(\text{II})$ cations were generated from their nitrate hydrates (Aldrich, p.a. $\geq 99.99\%$) without further purification; guanosine was purchased from SIGMA p.a. $\geq 98\%$. HPLC degree methanol and Millipore (18.2 M Ω cm) water were used to prepare the solvent mixture. Guanosine and the metal salt were dissolved in 1:3 water/methanol mixtures at concentrations of 200 and 100 μM , respectively.

3. Results and Discussion

Complexes of the type $[\text{Cu}(\text{L})_n]^{2+}$ were readily observed by electrospraying a solution containing appropriate amounts of copper(II) and the guanosine (L) molecules. The observed value of n depends on the magnitude of the declustering potential. Below 30 V, n typically is 4–6. At higher declustering potentials (above 50 V), the maximum value of n is reduced and charge reduction via interligand proton transfer, electron transfer, and other dissociation channels takes place in the source and leads to diversified MS products. The experiments reported here are performed primarily at low declustering potentials so as to promote the abundance of Cu–guanosine complex ions with large values of n , unless the CID of other derivative ions was of interest.

3.1. ESI-MS of Cu^{2+} /Guanosine Solutions. The ESI mass spectrum of guanosine in the presence of Cu^{II} (copper:guanosine molar ratio = 1:2) recorded at a low declustering potential (see Figure 1) showed several peaks at m/z 314.6, 456.0, 597.5, 739.0, and 880.3 corresponding to $[\text{CuL}_n]^{2+}$ ($n = 2-6$); 205.1 and 221.3 assigned to $[\text{Cu}(\text{L})(\text{MeOH})_{2,3}]^{2+}$; 407.8, 690.9, and 973.8 corresponding to $[\text{Cu}(\text{L})_n(\text{NO}_3)]^+$ ($n = 1-3$); 33.3 and 65.3 assigned to $[(\text{MeOH})_{1,2}\text{H}]^+$; 95.1 and 127.1 corresponding to $[\text{Cu}(\text{MeOH})_{1,2}]^+$; 126.1 and 158.1 assigned to $[\text{Cu}(\text{MeOH} - \text{H})(\text{MeOH})_{1-2}]^+$; 283.1 and 284.1 corresponding to $[\text{L}]^+$ and

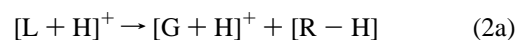
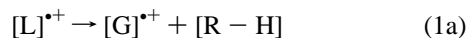
TABLE 1: Ion Distributions in the ESI-MS of a 1:3 Water/Methanol Solution of Copper(II) and Guanosine (L) at Low Declustering Potential (15 V)

main ion peak (m/z) ^a	assignment	relative peak intensity (%)
33.3	$[(\text{MeOH}) + \text{H}]^+$	12.1
65.3	$[(\text{MeOH})_2 + \text{H}]^+$	67.9
95.1	$[\text{Cu}(\text{MeOH})]^+$	7.9
133.1	$[\text{R}]^+$	14.4
151.3	$[\text{G}]^+$	12.3
152.1	$[\text{G} + \text{H}]^+$	12.8
126.1	$[\text{Cu}(\text{MeOH} - \text{H})(\text{MeOH})]^+$	60.7
127.1	$[\text{Cu}(\text{MeOH})_2]^+$	80.1
158.1	$[\text{Cu}(\text{MeOH} - \text{H})(\text{MeOH})_2]^+$	17.3
189.1	$[\text{Cu}(\text{NO}_3)(\text{MeOH})_2]^+$	12.8
205.1	$[\text{Cu}(\text{L})(\text{MeOH})_2]^{2+}$	21.7
221.3	$[\text{Cu}(\text{L})(\text{MeOH})_3]^{2+}$	10.5
283.1	$[\text{L}]^+$	100
284.1	$[\text{L} + \text{H}]^+$	54.4
314.6	$[\text{Cu}(\text{L})_2]^{2+}$	93.6
407.8	$[\text{Cu}(\text{L})(\text{NO}_3)]^+$	36.5
456.0	$[\text{Cu}(\text{L})_3]^{2+}$	25.9
495.9	$[\text{Cu}(\text{L})(\text{G}-\text{H})]^+$	6.8
597.5	$[\text{Cu}(\text{L})_4]^{2+}$	7.9
629.0	$[\text{Cu}(\text{L})_2]^+$	2.5
690.8	$[\text{Cu}(\text{L})_2(\text{NO}_3)]^+$	11.7
739.0	$[\text{Cu}(\text{L})_5]^{2+}$	1.8
880.3	$[\text{Cu}(\text{L})_6]^{2+}$	0.4
973.8	$[\text{Cu}(\text{L})_3(\text{NO}_3)]^+$	0.5

^a The ^{65}Cu complex peaks are not included.

$[\text{L} + \text{H}]^+$; 189.1, 133.1, 151.3, 152.1 assigned as $[\text{Cu}(\text{NO}_3)(\text{MeOH})_2]^+$, $[\text{R}]^+$ (R = ribose group), $[\text{G}]^+$, and $[\text{G} + \text{H}]^+$; and 495.9 and 629.0 corresponding to $[\text{Cu}(\text{L})(\text{G} - \text{H})]^+$ and $[\text{Cu}(\text{L})_2]^+$, respectively. The intensities in the ESI mass spectra of the mixture of Cu^{II} with guanosine normalized to the intensity of the radical guanosine cation peak are summarized in Table 1. The chemical compositions of ions were assigned and confirmed from isotopic patterns, especially for those that contain Cu. The two isotopes ^{63}Cu and ^{65}Cu have an abundance ratio of 69:31. The concentration dependence of the ESI mass spectrum was not investigated.

The observation of the large abundance of $[\text{L}]^+$ in the ESI-MS spectrum at low declustering potential was quite unexpected. The formation of $[\text{L}]^+$ can be achieved through the transfer of an electron from L to Cu^{2+} within the Cu–guanosine complex before Coulombic repulsion dissociates the complex into a singly charged Cu complex and $[\text{L}]^+$. However, the appearance of $[\text{L}]^+$ means that the intracomplex electron-transfer process can occur in the spray at low declustering potential. The formation of the observed $[\text{G}]^+$, $[\text{G} + \text{H}]^+$, and $[\text{R}]^+$ ions can proceed through the dissociation of the N–glycoside bond according to reactions 1 and 2.



Our measurements of the CIDs of $[\text{L}]^{\bullet+}$ and $[\text{L} + \text{H}]^+$ at low energies confirm the occurrence of these two processes (see Figure 2), but the formation of $[\text{R}]^+$ from the CID of $[\text{L}]^{\bullet+}$ and $[\text{L} + \text{H}]^+$ (channels 1b and 2b) is minor.

The observed $[\text{Cu}(\text{MeOH} - \text{H})(\text{MeOH})_{1-2}]^{\bullet+}$ ions can arise from collisional dissociation via reaction 3 after interligand

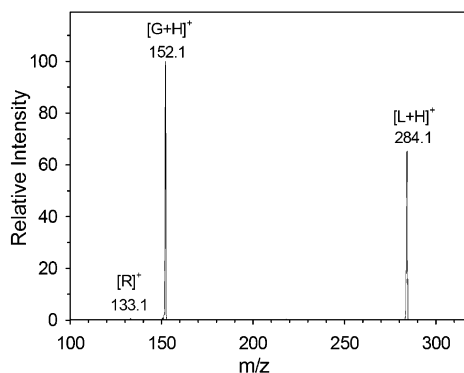
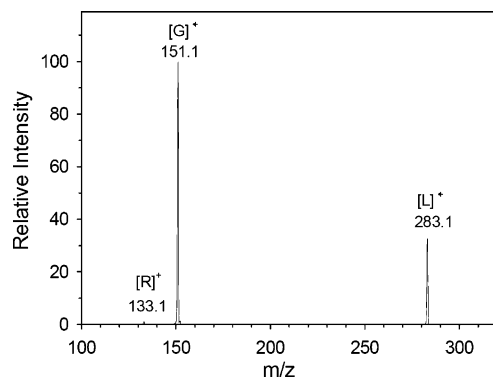


Figure 2. CID of (left) $[L]^+$ and (right) $[L+H]^+$ at $E_{\text{lab}} = 10$ eV.

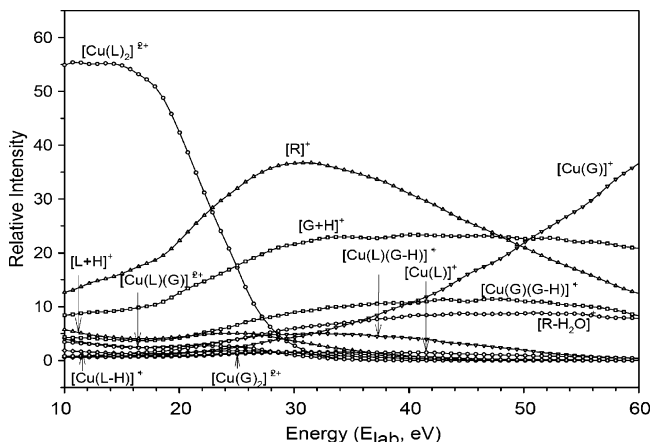
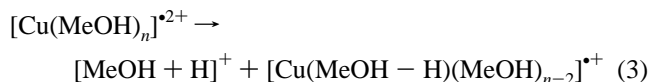


Figure 3. Breakdown curves for $[\text{Cu}(\text{L})_2]^{2+}$. Intensities are normalized to the sum of the intensities of the parent and product ions.

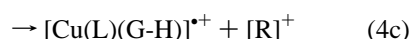
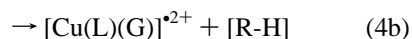
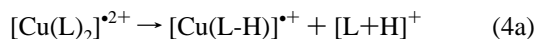
proton transfer within the Cu^{II} -methanol complexes $[\text{Cu}(\text{MeOH})_n]^{2+}$.



The observed $[\text{Cu}(\text{L})(\text{G} - \text{H})]^+$ and $[\text{Cu}(\text{L})_2]^+$ ions can be formed from the dissociation of the doubly charged copper-guanosine complexes, as discussed later.

Moriwaki²⁹ has studied the ESI-MS of complexes of Cd^{2+} with guanosine and saw the main peaks of $[\text{Cd}(\text{L})_n]^{2+}$ ($n = 2-8$) at a quite high ligand to metal cation molar ratio (9:1) at a cone potential of 20 V. This observation is very similar to our Cu -guanosine results; however, Moriwaki did not report the observation of guanosine radical cations, $[\text{L}]^+$.

3.2. CID of $[\text{Cu}(\text{L})_n]^{2+}$ ($n = 2-4$) Complexes. Figure 3 shows the breakdown curves for $[\text{Cu}(\text{L})_2]^{2+}$. Three primary fragmentation channels were identified as interligand proton transfer (PT) accompanied by dissociation to give $[\text{L} + \text{H}]^+$ and $[\text{Cu}(\text{L} - \text{H})]^+$, reaction 4a; loss of $[\text{R} - \text{H}]$ to produce $[\text{Cu}(\text{L})(\text{G})]^{2+}$, reaction 4b; and dissociative charge reduction (DCR) by breaking of the N-glycoside bond in one ligand to give $[\text{Cu}(\text{L})(\text{G} - \text{H})]^+$ and $[\text{R}]^+$, reaction 4c.



It is interesting to note that charge separation by electron transfer to give $[\text{Cu}(\text{L})]^+$ and the $[\text{L}]^+$ radical cation was not observed.

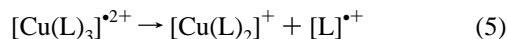
This may be a consequence of the high proton affinity of guanosine ($\text{PA} = 236.8 \text{ kcal mol}^{-1}$),⁴³ which may act to lower the energy barrier for intramolecular proton transfer below that for intramolecular electron transfer.

The CID spectrum of $[\text{Cu}(\text{L})(\text{G})]^{2+}$ (m/z 248.6) at a laboratory energy of 20 eV is shown in Figure 4a. Similar to the CID of $[\text{Cu}(\text{L})_2]^+$, three product channels were observed: intraligand proton transfer to produce $[\text{G} + \text{H}]^+$ (m/z 152.1) and $[\text{Cu}(\text{L} - \text{H})]^+$ (m/z 345.1), $[\text{R} - \text{H}]$ loss to produce $[\text{Cu}(\text{G})_2]^{2+}$ (m/z 182.6), and ligand dissociation/charge reduction to produce $[\text{Cu}(\text{G})(\text{G} - \text{H})]^+$ (m/z 364.0) and $[\text{R}]^+$.

The CID spectrum of $[\text{Cu}(\text{L})(\text{G} - \text{H})]^+$ (m/z 496.1) at a laboratory energy of 22 eV is shown in Figure 4b. Four dissociation channels were observed. The main channel is loss of $(\text{R} - \text{H})$ to produce $[\text{Cu}(\text{G})(\text{G} - \text{H})]^+$ (m/z 364.0); the second is loss of $(\text{G} - \text{H})^+$ to produce $[\text{Cu}(\text{L})]^+$ (m/z 346.0), and the other two channels involve the cleavage of the ribose ring to produce $[\text{Cu}(\text{G})(\text{G} - \text{H} + \text{COH})]^+$ (m/z 392.9) and $[\text{Cu}(\text{G})(\text{G} - \text{H} + \text{C}_2\text{H}_5\text{O})]^+$ (m/z 407.0). The CID spectra of $[\text{Cu}(\text{L})]^+$ (25 eV), $[\text{Cu}(\text{L} - \text{H})]^+$ (15 eV), and $[\text{Cu}(\text{G})(\text{G} - \text{H})]^+$ (22 eV) (where the laboratory collision energies are given in parentheses) are shown Figure 4c,d,e. The main dissociation product is $[\text{Cu}(\text{G})]^+$ with all three cations. Figure 4f shows the CID spectrum of $[\text{Cu}(\text{G})_2]^{2+}$ (34 eV) and in this case the main dissociation channel is electron transfer to produce $[\text{Cu}(\text{G})]^+$ and $[\text{G}]^+$, which is quite different from the CID of $[\text{Cu}(\text{L})_2]^{2+}$ and $[\text{Cu}(\text{L})(\text{G})]^{2+}$. Intramolecular electron transfer favors formation of $[\text{Cu}(\text{G})]^+$ presumably because of the lower proton affinity and ionization energy of G compared to L: $\text{PA}(\text{G}) = 229.4 \text{ kcal mol}^{-1}$,⁴⁴ $\text{IE}(\text{G}) = 7.85 \text{ eV}$ ⁴⁴ vs $\text{PA}(\text{L}) 236.8 \text{ kcal mol}^{-1}$,⁴³ $\text{IE}(\text{L}) = 8.0 \text{ eV}$.⁴⁵ This means that the nature of the R group may play a decisive role in the intramolecular proton transfer that accompanies the dissociation of $[\text{Cu}(\text{L})_2]^{2+}$ and $[\text{Cu}(\text{L})(\text{G})]^{2+}$.

A summary of the main fragmentation pathways for $[\text{Cu}(\text{L})_2]^{2+}$ and its product ions is shown in Scheme 1.

Figure 5 shows the CID spectrum of $[\text{Cu}(\text{L})_3]^{2+}$ at a laboratory energy of 24 eV, which is very different from that observed for $[\text{Cu}(\text{L})_2]^{2+}$. The three main reaction channels observed in the CID of $[\text{Cu}(\text{L})_2]^{2+}$ are all absent, and the charge separation reaction 5, which was not observed in the CID of $[\text{Cu}(\text{L})_2]^{2+}$, becomes the only dissociation channel.



Generally speaking, stabilization of a complex can be achieved by multiple ligation, which facilitates delocalization of the Cu^{2+} charges onto the ligands. However, the introduction of an additional ligand also increases the possibility of other competing dissociation pathways, such as proton transfer and

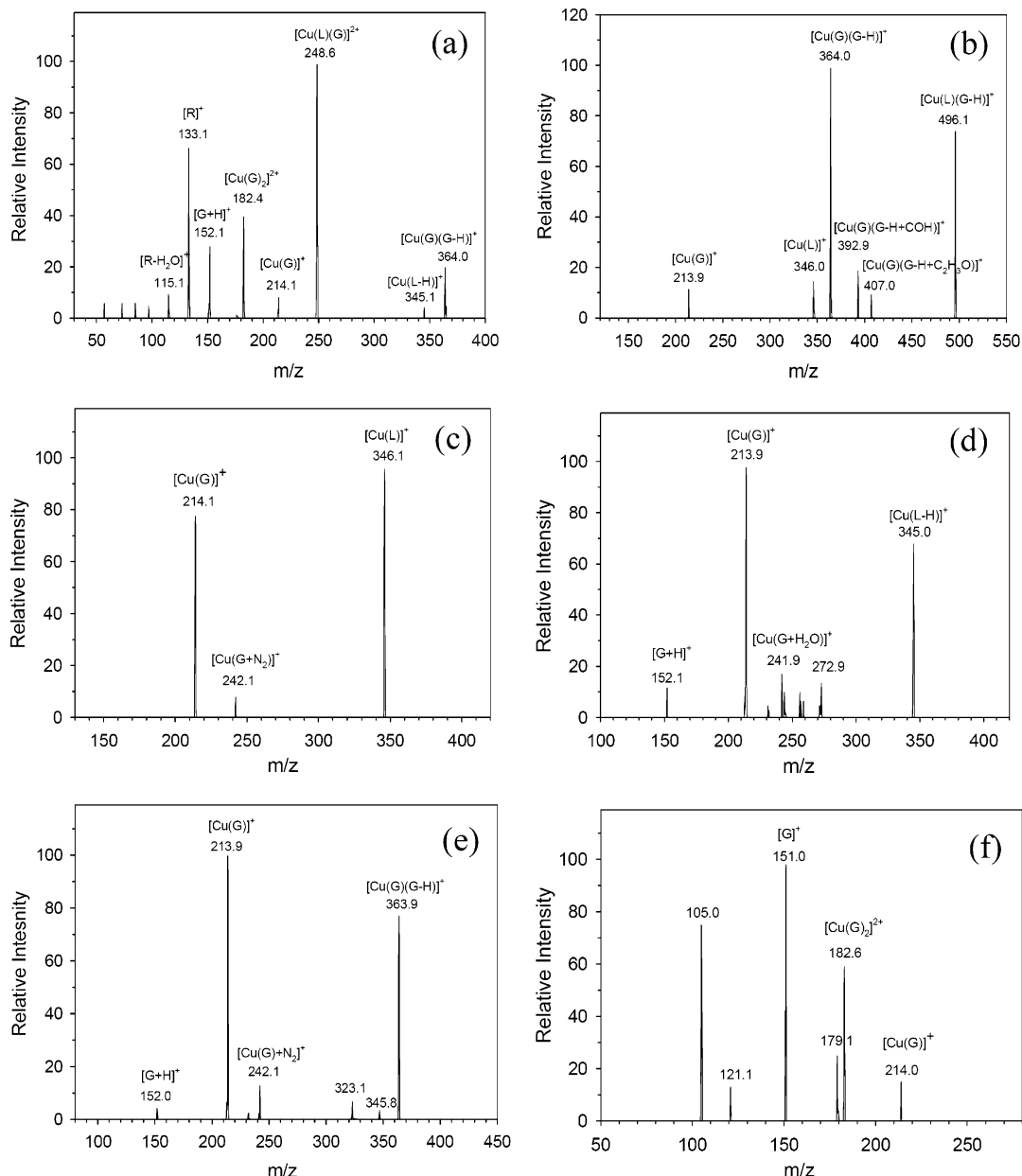


Figure 4. CID of (a) $[\text{Cu}(\text{L})(\text{G})]^{2+}$ at $E_{\text{lab}} = 20$ eV, (b) $[\text{Cu}(\text{L})(\text{G-H})]^+$ at $E_{\text{lab}} = 22$ eV, (c) $[\text{Cu}(\text{L})]^+$ at $E_{\text{lab}} = 25$ eV, (d) $[\text{Cu}(\text{L-H})]^+$ at $E_{\text{lab}} = 15$ eV, (e) $[\text{Cu}(\text{G})(\text{G-H})]^+$ at $E_{\text{lab}} = 22$ eV, and (f) $[\text{Cu}(\text{G})_2]^{2+}$ at $E_{\text{lab}} = 34$ eV. In part f, the m/z 105 ion probably is $[\text{CuCN}_2\text{H}_2]^+$, which might arise from the dissociation of the 5-membered ring of $[\text{Cu}(\text{G})]^+$, and 121 might be $[\text{CuCN}_3\text{H}_4]^+$; m/z 179 probably is $[\text{G}]^+(\text{N}_2)$.

SCHEME 1

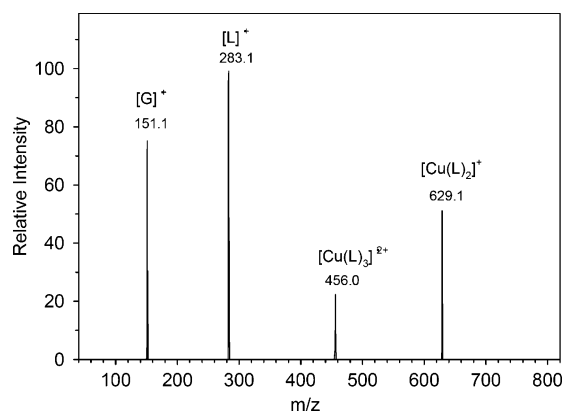
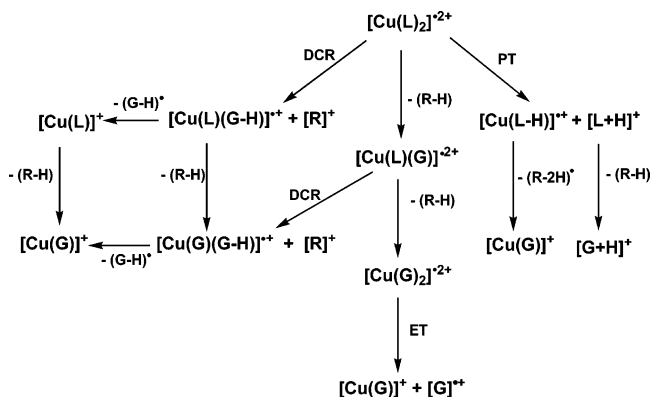


Figure 5. CID of $[\text{Cu}(\text{L})_3]^{2+}$ at $E_{\text{lab}} = 24$ eV.

neutral ligand loss. So it is quite interesting to see from the CID results for $[\text{Cu}(\text{L})_2]^{2+}$ and $[\text{Cu}(\text{L})_3]^{2+}$ that the original channels all disappear and a new electron-transfer pathway

dominates with the addition of the third ligand. Electron transfer according to reaction 5 reduces Cu(II) to Cu(I), which bonds strongly to two ligands according to previous measurements of

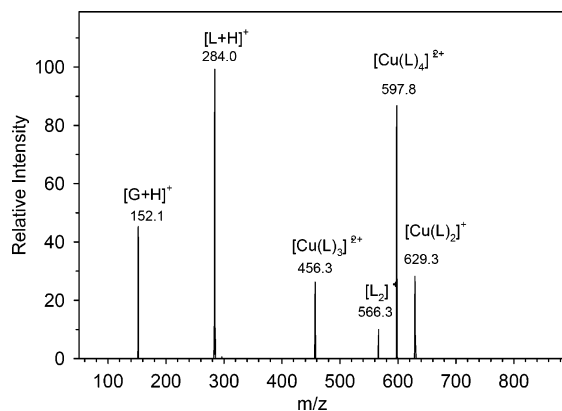


Figure 6. CID of $[\text{Cu}(\text{L})_4]^{2+}$ at $E_{\text{lab}} = 32$ eV.

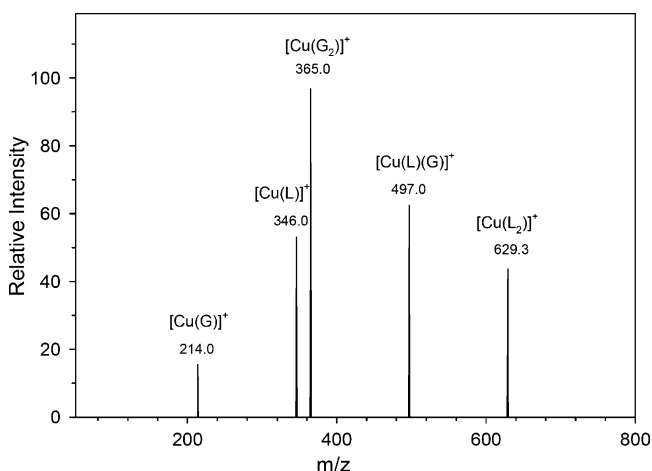
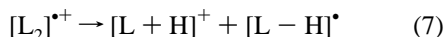
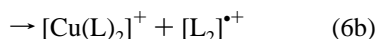
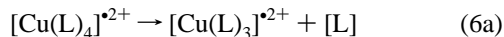


Figure 7. CID of $[\text{Cu}(\text{L})_2]^+$ at $E_{\text{lab}} = 35$ eV.

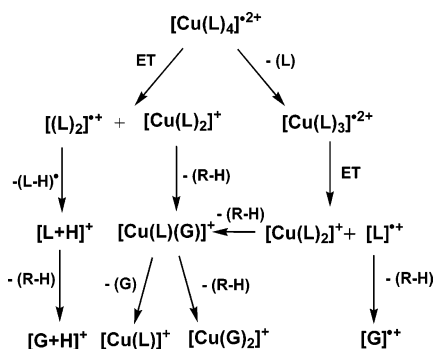
the binding energies of Cu^+ with various ligands such as imidazole,⁴⁶ $(\text{CH}_3)_2\text{CO}$,⁴⁷ CH_3CN ,⁴⁸ H_2O ,⁴⁹ NH_3 ,⁵⁰ and $\text{CH}_3\text{-OCH}_3$.⁵¹ A sharp decrease occurs in the binding energy of the third ligand.

The CID spectrum of $[\text{Cu}(\text{L})_4]^{2+}$ (m/z 597.8) at a laboratory energy of 32 eV is shown in Figure 6. There are six peaks in this spectrum: m/z 152.0 $[\text{G} + \text{H}]^+$, m/z 284.0 $[\text{L} + \text{H}]^+$, m/z 456.7 $[\text{CuL}_3]^{2+}$, m/z 566.3 $[\text{L}_2]^{2+}$, m/z 597.8 $[\text{Cu}(\text{L})_4]^{2+}$, and m/z 629.0 $[\text{Cu}(\text{L})_2]^+$. At least two primary dissociation channels can be identified: loss of a neutral ligand to form $[\text{Cu}(\text{L})_3]^{2+}$ (reaction 6a) and intramolecular electron transfer to form $[\text{L}_2]^{2+}$ and $[\text{Cu}(\text{L})_2]^+$ (reaction 6b). The large $[\text{L} + \text{H}]^+$ is attributed to the dissociation of $[\text{L}_2]^{2+}$ (reaction 7), although the CID of $[\text{L}_2]^{2+}$ could not be measured separately. $[\text{L} + \text{H}]^+$ cannot arise from the dissociative charge separation of $[\text{Cu}(\text{L})_4]^{2+}$ since we did not see the accompanying $[\text{Cu}(\text{L} - \text{H})\text{L}_2]^{2+}$ ion and also is not a dissociation product of $[\text{Cu}(\text{L})_2]^+$. The CID spectrum of $[\text{Cu}(\text{L})_2]^+$ at a laboratory energy of 35 V is presented in Figure 7 and shows a primary CID channel that corresponds to the loss of $[\text{R} - \text{H}]$ to produce $[\text{Cu}(\text{L})(\text{G})]^+$ (m/z 497.0). At higher energies the $[\text{Cu}(\text{L})(\text{G})]^+$ continues to lose $[\text{R} - \text{H}]$ and $[\text{G}]$ to produce $[\text{Cu}(\text{G}_2)]^+$ (m/z 365.0) and $[\text{Cu}(\text{L})]^+$ (m/z 346.1).

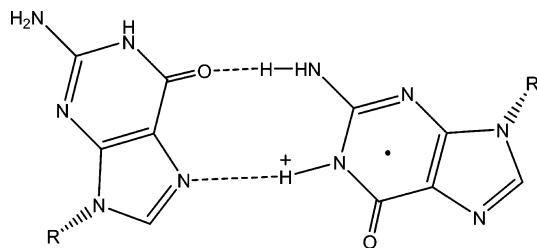


The overall dissociation pathway proposed for $[\text{Cu}(\text{L})_4]^{2+}$ is presented in Scheme 2.

SCHEME 2



SCHEME 3



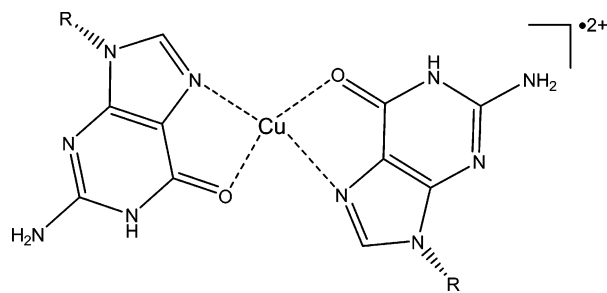
A likely structure of the radical dimer cation is shown in Scheme 3 in which the two ligands are connected with both a proton and a hydrogen bond bridge. The CID of $[\text{L}_2]^{2+}$ to produce $[\text{L} + \text{H}]^+$ and $[\text{L} - \text{H}]^+$ can be regarded as a competition between the $[\text{L}]$ and $[\text{L} - \text{H}]^+$ for a proton. And it is quite reasonable to suggest that a proton bridge may exist between them. The suggested dissociation implies that $\text{PA}(\text{L}) > \text{PA}([\text{L} - \text{H}]^+)$.

A number of previous mass spectrometric studies have shown that complexes of oligomeric nucleosides can be formed with singly charged metal ions, for example, $\text{Na}^+ - (\text{G-quartet})$ for guanosine, and that singly charged complexes of alkali ions with nucleosides and nucleoside bases exhibit several magic numbers.^{52,53} The major interactions in the clusters of deoxyguanosine or guanosine appear to be those between the nucleobases and not the sugar residues; however, the formation of metal clusters may be favored by interactions with the sugars.⁵³ Metal binding is known to promote the formation of hydrogen-bonded complexes of nucleic acids.⁵⁴ Guanosine derivatives exhibit a range of supramolecular architectures, including templated tetramers and two ribbon structures.⁵⁵

A recent report³⁰ on the interaction of singly and doubly charged metal cations with cytidine indicates that cytidine molecules aggregate around alkali and alkaline earth metal cations through electrostatic interaction, while in the presence of other divalent cations (with 3d electrons), the interaction can be regarded as coordination to the metal cations. Similar coordination may occur in $\text{Cu}(\text{II})$ -guanosine complexes.

It is well-known that the N7 position of guanine, which is readily accessible in the major groove of duplex DNA and is not involved in Watson-Crick base pairing, and the O6 position are the preferred metal binding sites.^{2,56,57} The carbonyl and hydroxyl oxygen atoms in the ribose group also are possible metal-coordinating sites in the formation of complexes with guanosine. Generally, copper(II) prefers a coordination number of 4, and a square-planar or octahedral geometry when coordinating with ligands.^{58,59} We did not observe a ribose ring cleavage channel in our CID experiment with $[\text{Cu}(\text{L})_2]^{2+}$, but we did see the sequential loss of $(\text{R} - \text{H})$ groups to form $[\text{Cu}(\text{G}_2)]^{2+}$. And it is quite reasonable that the ribose group is not involved in binding with the metal cations.

SCHEME 4



We also tried the ESI of Cu^{2+} and guanine solution with the same concentration and operating conditions as Cu^{2+} and guanosine. The doubly charged complexes, $[\text{Cu}(\text{G})_n]^{2+}$, were not observed. In the CID of $[\text{Cu}(\text{G})_2]^{2+}$, electron transfer to produce the $[\text{G}]^+$ and $[\text{Cu}(\text{G})]^+$ was the main channel and the proton-transfer channel that was seen in the CID of $[\text{Cu}(\text{L})_2]^{2+}$ and $[\text{Cu}(\text{L})(\text{G})]^{2+}$ was not observed. Accordingly, we suggest that copper(II) cations only coordinate with guanosine base in $[\text{Cu}(\text{L})_2]^{2+}$, to form a square-planar structure (Scheme 4), and that the ribose group plays an important role in the stabilization of the complex and donates the proton in interligand proton transfer. It is interesting to note that previous IR spectrophotometry results⁶⁰ obtained for complexes of the type $[\text{ML}_2]^{n+}$ with $\text{M} = \text{U}(\text{VI}), \text{Th}(\text{IV}), \text{Ce}(\text{III}),$ and $\text{La}(\text{III})$, and $\text{L} = \text{cytidine}$, indicated that the metal cations only bind to the two cytidine bases of N3 and O2 simultaneously.

Giorgi et al.⁶¹ have investigated the structure of the guanosine clusters. They found that the lipophilic guanosine could be self-assembled into ribbonlike aggregates through hydrogen bonds, both in the crystal state and in solution. O'Hair et al.⁴⁰ prefer that $[\text{Pt}(\text{tpy})(\text{dG})_n]^{2+}$ ($\text{tpy} = 2,2':6',2''\text{-terpyridine}$, $\text{dG} = 2'\text{-deoxyguanosine}$, $n = 1-13$) adopts a ribbon structure in the gas phase. Moriwaki²⁹ prefers the structure of $[\text{Cd}(\text{L})_n]^{2+}$ to be the hydrogen-bonded square guanosine quartet, but the reasons seem incomplete. On the basis of our observation of intramolecular electron transfer rather than neutral ligand loss, we prefer a structure for $\text{Cu}(\text{L})_3^{2+}$ in which the third ligand loosely coordinates with the $\text{Cu}(\text{II})$ at N7 and also interacts with the other two ligands by hydrogen bonds or electrostatics. For the structure of $[\text{Cu}(\text{L})_n]^{2+}$ ($n \geq 4$), we expect that the extra ligands will connect sequentially with the three ligands by hydrogen bonds. Ke et al.⁴¹ also suggest that the first two ligands bind strongly with the $\text{Cu}(\text{II})$, and that the third and fourth ligands bind much more weakly in the complexes $[\text{Cu}(\text{M})_4]^{2+}$ ($\text{M} = \text{Ac-Trp-NH}_2$ and Ac-Trp-OMe). This is given as the likely reason for the formation of $[\text{M}_2]^{+}$ in the CID of $[\text{Cu}(\text{M})_4]^{2+}$.

3.3. CID of $[\text{Cu}(\text{L})(\text{MeOH})_{1-2}]^{2+}$ ($n = 2-4$) Complexes. The methanol molecule also was observed to be involved in complex formation. Complex cations of the type $[\text{Cu}(\text{L})(\text{MeOH})_{2-3}]^{2+}$ were found in the ESI-MS spectrum of mixtures of Cu^{2+} and guanosine dissolved in a water/methanol solution. The CID spectra of $[\text{Cu}(\text{L})(\text{MeOH})_{2,3}]^{2+}$ (m/z 205.1 and 221.1) at a laboratory energy of 10 eV are shown in Figure 8, parts a and b.

Two channels are observed in the dissociation of $[\text{Cu}(\text{L})(\text{MeOH})_2]^{2+}$: formation of the radical cation $[\text{L}]^+$ and $[\text{Cu}(\text{MeOH})_2]^+$ via intramolecular electron transfer (reaction 8a), and loss of neutral MeOH (reaction 8b) to form $[\text{Cu}(\text{L})(\text{MeOH})]^{2+}$, which easily dissociates further to form $[\text{Cu}(\text{G}-\text{H})(\text{MeOH})]^+$ and $[\text{R}]^+$ (reaction 9). Probably, the dissociation of $[\text{Cu}(\text{L})(\text{MeOH})]^{2+}$ can also produce the radical cation $[\text{L}]^+$ through reaction 10, but this cannot be confirmed on the basis of our observations and working conditions. The

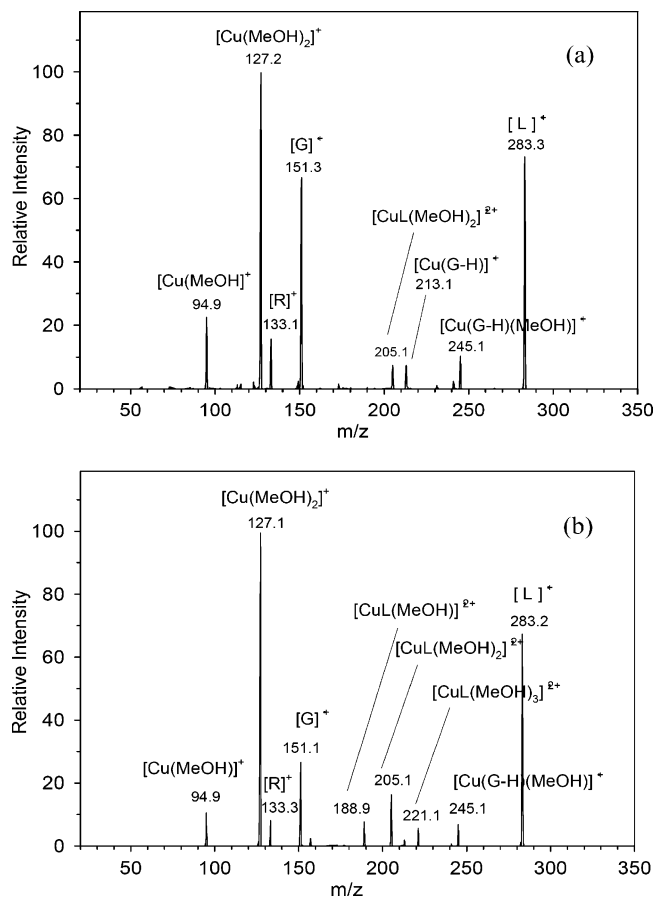
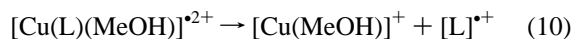
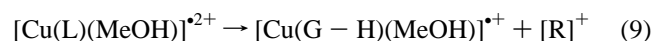
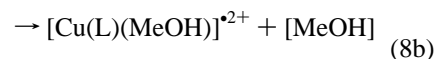
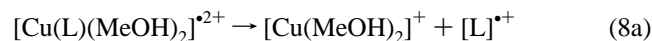


Figure 8. CID of (a) $[\text{Cu}(\text{L})(\text{MeOH})_2]^{2+}$ and (b) $[\text{Cu}(\text{L})(\text{MeOH})_3]^{2+}$ at $E_{\text{lab}} = 10$ eV.

binding of L and MeOH to $\text{Cu}(\text{II})$ seems to be so weak that we cannot observe their complex in the CID of $[\text{Cu}(\text{L})(\text{MeOH})_2]^{2+}$ even under the lowest CID energy of 10 eV; it appeared only in the 10 eV CID spectrum of $[\text{Cu}(\text{L})(\text{MeOH})_3]^{2+}$.



The CID spectrum of $[\text{Cu}(\text{L})(\text{MeOH})_3]^{2+}$ is very similar to that of $[\text{Cu}(\text{L})(\text{MeOH})_2]^{2+}$ and loss of MeOH was again observed (reaction 11).



Scheme 5 is a summary of the fragmentation pathways observed for $[\text{Cu}(\text{L})(\text{MeOH})_3]^{2+}$.

On the basis of the coordination properties of $\text{Cu}(\text{II})$ and guanosine that were already discussed, we think that $\text{Cu}(\text{II})$ in $[\text{Cu}(\text{L})(\text{MeOH})_2]^{2+}$ has a coordination number of 4 and binds at the N7 and O6 positions of guanosine and the O-atoms of the two methanol molecules. In $[\text{Cu}(\text{L})(\text{MeOH})_3]^{2+}$ the $\text{Cu}(\text{II})$ will show a coordination number of 5 in binding with the guanosine and the methanol molecules, but the binding with the third methanol molecule is not as strong as that with the first two, which makes the peak of $[\text{Cu}(\text{L})(\text{MeOH})_3]^{2+}$ (m/z 221.3) much lower than that of $[\text{Cu}(\text{L})(\text{MeOH})_2]^{2+}$ (m/z 205.1)

SCHEME 5

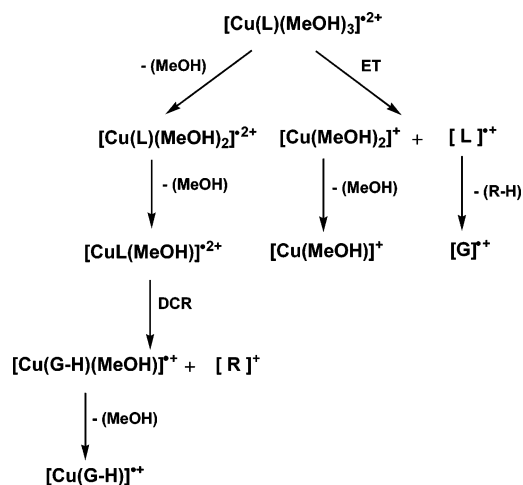


TABLE 2: Summary of the Predominant Primary Product Ions Formed by Intramolecular Electron and Proton Transfer in the CID of Doubly Charged Metal-Complex Cations with L = Guanosine and G = Guanine

metal-complex cations	[L] ^{•+}	[L ₂] ^{•+}	[L + H] ⁺	[G] ^{•+}	[G + H] ⁺
[Cu(L) ₂] ²⁺			*		
[Cu(L)(G)] ²⁺					*
[Cu(G) ₂] ²⁺				*	
[Cu(L) ₃] ²⁺	*				
[Cu(L) ₄] ²⁺		*			
[Cu(L)(MeOH) ₂] ²⁺	*				

TABLE 3: Summary of Primary Channels in the CID of Doubly Charged Metal-Complex Cations That Lead to the Formation of Cationic Ligand Radicals with G = Guanine and L = Guanosine

reaction	dissociation type
[Cu(G) ₂] ²⁺ → [Cu(G)] ⁺ + [G] ^{•+}	ET
[Cu(L) ₃] ²⁺ → [Cu(L) ₂] ⁺ + [L] ^{•+}	ET
[Cu(L)(MeOH) ₂] ²⁺ → [Cu(MeOH) ₂] ⁺ + [L] ^{•+}	ET
[Cu(L) ₄] ²⁺ → [Cu(L) ₂] ⁺ + [L ₂] ^{•+}	ET

(see Figure 1). The formation of [L]^{•+} from [Cu(L)(MeOH)₂]²⁺ is likely to be favored from the low ionization energy of L and the high stability of the product ion [Cu(MeOH)₂]⁺.^{45,46}

The ESI-MS/MS of the ternary copper(II) doubly charged complex, [Cu(L)(M)]²⁺, to produce radical cations has been investigated quite often and the types of fragmentation that were observed for these complexes depend on the nature of the ligands L and M.^{36–39}

Compared to [Cu(L)₂]²⁺, the complex [Cu(L)(MeOH)_{2–3}]²⁺ ions are much easier to dissociate to produce the molecular radical cations [L]^{•+} (see Figures 6 and 8). The large abundance of the radical cations [L]^{•+} in the ESI-MS spectrum of guanosine and Cu^{II} solutions at low declustering potential would be mostly due to the dissociation of [Cu(L)(MeOH)_{2,3}]²⁺.

Intramolecular ET and PT are the main primary CID channels that were observed for the CID of the doubly charged cations investigated in the experiments reported here. Table 2 provides a list the product ions formed by intramolecular ET and PT. Intramolecular PT was observed in the CID of [Cu(L)₂]²⁺ and [Cu(L)(G)]²⁺. Intramolecular ET is observed for four ions, [Cu(G)₂]²⁺, [Cu(L)₃]²⁺, [Cu(L)₄]²⁺, and [Cu(L)(MeOH)₂]²⁺, and the reactions are summarized in Table 3.

4. Conclusions

Doubly charged Cu complexes, [CuL_n]²⁺ and [CuL(MeOH)_n]²⁺, and other ions, [L]^{•+}, [L + H]⁺, [G]^{•+}, etc., are formed in the electrospray of water and methanol solutions of Cu(NO₃)₂ and guanosine. CID experiments indicate that the guanosine radical cation [L]^{•+} is generated by the dissociations of [CuL₃]²⁺ and [CuL(MeOH)_n]²⁺ (n = 2, 3) and that the dimeric guanosine radical cation, [L₂]^{•+}, is generated by the dissociation of [CuL₄]²⁺. For [CuL₂]²⁺, the dissociation channel is interligand proton transfer to produce protonated guanosine [L + H]⁺, and the radical cation [G]^{•+} can be produced in the CID of the higher order product [Cu(G)₂]²⁺. The structure of [L₂]^{•+} is proposed to involve interactions of two guanosines via proton and hydrogen bonding, and can be dissociated into [L + H]⁺ and [L – H][•] at relatively low dissociation energies. It is believed that the first two ligands bind strongly with Cu(II) to form a four-coordinated planar complex [CuL₂]²⁺, and a third ligand will bind loosely with copper in [CuL₃]²⁺. The extra ligands are supposed to sequentially bind with the first three ligands by hydrogen bonding to form [CuL_n]²⁺ (n ≥ 4). The ribose group may play an important role in complex stabilization by interligand proton transfer.

Acknowledgment. Continued financial support from the Natural Sciences and Engineering Research Council of Canada is greatly appreciated. Also, we acknowledge support from the National Research Council, the Natural Science and Engineering Research Council, and MDS SCIEX in the form of a Research Partnership grant. As holder of a Canada Research Chair in Physical Chemistry, Diethard K. Bohme thanks the contributions of the Canada Research Chair Program to this research.

References and Notes

- (1) Sigel, A.; Sigel, H., Eds. *Probing of Nucleic Acids by Metal Ion Complexes of Small Molecules*; Metal Ions in Biological Systems, Vol. 33; Dekker: New York, 1996.
- (2) Lippert, B. *Coord. Chem. Rev.* **2000**, 200–202, 487.
- (3) Burrows, C. J.; Muller, J. G. *Chem. Rev.* **1998**, 98, 1109.
- (4) Harford, C.; Sarkar, B. *Acc. Chem. Res.* **1997**, 30, 123.
- (5) Theophanides, T.; Bariyanga, J. *J. Mol. Struct.* **1989**, 214, 177.
- (6) Marino, T.; Toscano, M.; Russo, N.; Grand, A. *Int. J. Quantum Chem.* **2004**, 98, 347.
- (7) Drouin, R.; Rodriguez, H.; Gao, S. W.; Gebreyes, Z.; O'Connor, T. R.; Holmquist, G. P.; Akman, S. A. *Free Radical Biol. Med.* **1996**, 21, 261.
- (8) Halliwell, B.; Aruoma, O. I. *FEBS Lett.* **1991**, 281, 9.
- (9) Lomozik, L.; Gasowska, A.; Bregier-Jarzebowska, R.; Jastrzab, R. *Coord. Chem. Rev.* **2005**, 249, 2335.
- (10) Sigel, H. *J. Inorg. Nucl. Chem.* **1977**, 39, 1903.
- (11) Sigel, H.; Fischer, B. E.; Priejs, B. *J. Am. Chem. Soc.* **1977**, 99, 4489.
- (12) Knobloch, B.; Sigel, H. *JBIC, J. Biol. Inorg. Chem.* **2004**, 9, 365.
- (13) Sigel, H.; Da Costa, C. P.; Martin, R. B. *Coord. Chem. Rev.* **2001**, 219–221, 435.
- (14) Swiatek-Kozłowska, J.; Brasun, J.; Dobosz, A.; Sochacka, E.; Glowacka, A. *J. Inorg. Biochem.* **2003**, 93, 119.
- (15) Blades, A. T.; Jayaweera, P.; Ikononou, M. G.; Kebarle, P. *J. Chem. Phys.* **1990**, 92, 5900.
- (16) Blades, A. T.; Jayaweera, P.; Ikononou, M. G.; Kebarle, P. *Int. J. Mass Spectrom. Ion Processes* **1990**, 102, 251.
- (17) Spence, T. G.; Burns, T. D.; Posey, L. A. *J. Phys. Chem. A* **1997**, 101, 139.
- (18) Peschke, M.; Blades, A. T.; Kebarle, P. *J. Am. Chem. Soc.* **2000**, 122, 10440.
- (19) Rodriguez-Cruz, S. E.; Jockusch, R. A.; Williams, E. R. *J. Am. Chem. Soc.* **1998**, 120, 5842.
- (20) Stone, J. A.; Vukomanovic, D. *Chem. Phys. Lett.* **2001**, 346, 419.
- (21) Shvartsburg, A. A.; Siu, K. W. M. *J. Am. Chem. Soc.* **2001**, 123, 10071.
- (22) Peschke, M.; Blades, A. T.; Kebarle, P. *J. Am. Chem. Soc.* **2000**, 122, 1492.
- (23) Cheng, Z. L.; Siu, K. W. M.; Guevremont, R.; Berman, S. S. *Org. Mass Spectrom.* **1992**, 27, 1370.

- (24) Kohler, M.; Leary, J. A. *J. Am. Soc. Mass Spectrom.* **1997**, *8*, 1124.
- (25) Andersen, U. N.; Bojesen, G. *Int. J. Mass Spectrom. Ion Processes* **1996**, *153*, 1.
- (26) Hall, B. J.; Brodbelt, J. S. *J. Am. Soc. Mass Spectrom.* **1999**, *10*, 402.
- (27) Shvartsburg, A. A.; Wilkes, J. G.; Lay, J. O.; Siu, K. W. M. *Chem. Phys. Lett.* **2001**, *350*, 216.
- (28) Jayaweera, P.; Blades, A. T.; Ikonou, M. G.; Kebarle, P. *J. Am. Chem. Soc.* **1990**, *112*, 2452.
- (29) Moriwaki, H. *J. Mass Spectrom.* **2003**, *38*, 321.
- (30) Mochizuki, S.; Wakisaka, A. *J. Phys. Chem. B* **2003**, *107*, 5612.
- (31) Moroni, F.; Famulari, A.; Raimondi, M.; Sabat, M. *J. Phys. Chem. B* **2003**, *107*, 4196.
- (32) Baker, E. S.; Bernstein, S. L.; Bowers, M. T. *J. Am. Soc. Mass Spectrom.* **2005**, *16*, 989.
- (33) Guillaumont, S.; Tortajada, J.; Salpin, J.-Y.; Lamsabhi, A. M. *Int. J. Mass Spectrom.* **2005**, *243*, 279.
- (34) Noguera, M.; Sodupe, M.; Bertran, J. *Theor. Chem. Acc.* **2004**, *112*, 318.
- (35) Tao, W. A.; Zhang, D.; Nikolaev, E. N.; Cooks, R. G. *J. Am. Chem. Soc.* **2000**, *122*, 10598.
- (36) Chu, I. K.; Rodriguez, C. F.; Lau, T.-C.; Hopkinson, A. C.; Siu, K. W. M. *J. Phys. Chem. B* **2000**, *104*, 3393.
- (37) Chu, I. K.; Rodriguez, C. F.; Hopkinson, A. C.; Siu, K. W.; Lau, T. C. *J. Am. Soc. Mass Spectrom.* **2001**, *12*, 1114.
- (38) Bagheri-Majidi, E.; Ke, Y.; Orlova, G.; Chu, I. K.; Hopkinson, A. C.; Siu, K. W. M. *J. Phys. Chem. B* **2004**, *108*, 11170.
- (39) Chu, I. K.; Siu, S. O.; Lam, C. N. W.; Chan, J. C. Y.; Rodriguez, C. F. *Rapid Commun. Mass Spectrom.* **2004**, *18*, 1798.
- (40) Wee, S.; O'Hair, R. A. J.; McFadyen, W. D. *Rapid Commun. Mass Spectrom.* **2005**, *19*, 1797.
- (41) Ke, Y.; Verkerk, U. H.; Shek, P. Y. I.; Hopkinson, A. C.; Siu, K. W. M. *J. Phys. Chem. B* **2006**, *110*, 8517.
- (42) Anichina, J.; Zhao, X.; Bohme, D. K. *J. Phys. Chem. A* **2006**, *110*, 10763.
- (43) Di Donna, L.; Napoli, A.; Sindona, G.; Athanassopoulos, C. *J. Am. Soc. Mass Spectrom.* **2004**, *15*, 1080.
- (44) <http://webbook.nist.gov/chemistry/>.
- (45) Yu, C.; O'Donnell, T. J.; LeBreton, P. R. *J. Phys. Chem.* **1981**, *85*, 3851.
- (46) Rannulu, N. S.; Rodgers, M. T. *Phys. Chem. Chem. Phys.* **2005**, *7*, 1014.
- (47) Chu, Y.; Yang, Z.; Rodgers, M. T. *J. Am. Soc. Mass Spectrom.* **2002**, *13*, 453.
- (48) Vitale, G.; Valina, A. B.; Huang, H.; Amunugama, R.; Rodgers, M. T. *J. Phys. Chem. A* **2001**, *105*, 11351.
- (49) Dalleska, N. F.; Honma, K.; Sunderlin, L. S.; Armentrout, P. B. *J. Am. Chem. Soc.* **1994**, *116*, 3519.
- (50) Walter, D.; Armentrout, P. B. *J. Am. Chem. Soc.* **1998**, *120*, 3176.
- (51) Koizumi, H.; Zhang, X.-G.; Armentrout, P. B. *J. Phys. Chem. A* **2001**, *105*, 2444.
- (52) Koch, K. J.; Aggerholm, T.; Nanita, S. C.; Cooks, R. G. *J. Mass Spectrom.* **2002**, *37*, 676.
- (53) Aggerholm, T.; Nanita, S. C.; Koch, K. J.; Cooks, R. G. *J. Mass Spectrom.* **2003**, *38*, 87.
- (54) Navarro, J. A. R.; Lippert, B. *Coord. Chem. Rev.* **1999**, *185–186*, 653.
- (55) Davis, J. T. *Angew. Chem., Int. Ed.* **2004**, *43*, 668.
- (56) Burda, J. V.; Sponer, J.; Hobza, P. *J. Phys. Chem.* **1996**, *100*, 7250.
- (57) Burkitt, M. J. *Methods Enzymol.* **1994**, *234*, 66.
- (58) Lavanant, H.; Hecquet, E.; Hoppilliard, Y. *Int. J. Mass Spectrom.* **1999**, *185/186/187*, 11.
- (59) Wright, R. R.; Walker, N. R.; Firth, S.; Stace, A. J. *J. Phys. Chem. A* **2001**, *105*, 54.
- (60) Temerk, Y. M.; Kamal, M. M.; Ahmed, M. E.; Abd-El-Hamid, M. I. *Bioelectrochem. Bioenerg.* **1984**, *12*, 475.
- (61) Giorgi, T.; Grepioni, F.; Manet, I.; Mariani, P.; Masiero, S.; Mezzina, E.; Pieraccini, S.; Saturni, L.; Spada, G. P.; Gottarelli, G. *Chem. Eur. J.* **2002**, *8*, 2143.